

BITLIS EREN ÜNIVERSITESI FEN BİLİMLERİ DERGİSİ



ISSN: 2147-3129 / e-ISSN: 2147-3188

Article Type: Research Article : May 16, 2025 Received : September 22, 2025 Revised Accepted : September 27, 2025

: 10.17798/bitlisfen.1698675 DOI

Year :2025 :14 Volume Issue :3

: 1688-1701 **Pages**



THE EFFECT OF BORIDING ON THE WEAR BEHAVIOR OF AISI 8620 STEEL

Selcuk ATASOY 1 , Hasan Onur TAN 1, * , Hakan ADATEPE 1 , Sitki AKTAŞ 1 ,

İbrahim GÜNES ²

¹ Giresun University, Mechanical Engineering Department, Giresun, Türkiye

² Giresun University, Civil Engineering Department, Giresun, Türkiye

* Corresponding Author: hasan.tan@giresun.edu.tr

ABSTRACT

In this study, AISI 8620 steel-commonly used in the gear manufacturing industry—was subjected to a box boriding treatment using commercial Ekabor II powder. The process was carried out in an electric resistance furnace at 900 °C for a duration of 5 hours. The resulting boride layers were characterized using optical microscopy, X-ray diffraction (XRD), microhardness measurements, scanning electron microscopy (SEM), and energy-dispersive Xray spectroscopy (EDX). A boride layer with an average thickness of $78 \pm 2 \,\mu m$ was formed on the steel surface, consisting primarily of FeB and Fe2B phases, and the surface hardness reached 1768 HV_{0.05}. The wear tests were conducted under dry sliding conditions using a ball-on-disk setup at room temperature. The experiments were performed under a constant normal load of 10 N, at rotational speeds of 300, 450, and 600 rpm, over sliding distances of 250, 500, 750, 1000, 1500, and 2000 m. The coefficient of friction ranged between 0.40 and 0.62 throughout the tests. At higher rotational speeds, a reduction in the friction coefficient was observed up to 1000 meters, after which a gradual increase occurred at longer distances. Both the sliding distance and speed significantly affected the wear behavior, resulting in an increased wear track depth and wear rate. The wear rate was found to vary between 14.52×10^{-5} and $198.82 \times 10^{-5} \, \text{mm}^{3} \text{N}^{-1} \text{m}^{-1}$.

Boriding, Gear steel, Sliding distance, Wear rate, Friction coefficient. **Keywords:**

1 INTRODUCTION

AISI 8620 steel is a low-alloy carburizing steel that is widely used in critical machine components such as gears, shafts, camshafts, and bearings, where high core toughness and surface hardness are required[1-7]. This material is particularly favored in automotive and industrial equipment for dynamically loaded parts due to its balanced strength and machinability [4, 5, 8-10]. However, under high contact pressure and abrasive conditions, the wear resistance of this steel may prove inadequate, leading to premature component failure and limiting its applicability in more demanding service environments. This presents a significant issue in industrial applications in terms of performance and durability. Therefore, a better understanding of the material's mechanical strength, impact resistance, and other properties is crucial for enhancing its performance, ensuring reliability, and expanding its range of applications [4, 5, 7, 10-16].

The development of wear-resistant materials is vital for increasing the operational efficiency and reducing the maintenance costs. Material loss, increased energy consumption, and production downtimes are chain effects that result in billions of dollars in annual economic losses across industries. In high-precision sectors such as the automotive and aerospace industries, preventing wear-induced failures has become a critical goal for sustainability and cost optimization. For this reason, investigating and implementing technologies that improve the surface properties of existing materials is of great industrial relevance [5, 6, 17].

The wear resistance of AISI 8620 steel can be significantly improved through various surface modifications and treatment methods. These techniques primarily focus on altering the surface microstructure and composition to increase hardness and reduce wear. Common techniques include thermochemical treatments, surface alloying, carburizing, laser surface processing, and electro-mechanical hardening[1, 2, 7, 10, 12, 13, 16, 18]. For instance, Triani et al. demonstrated that thermochemical treatments at 1000°C produced vanadium and niobium carbide (VC and NbC) layers on AISI 8620 steel, significantly improving its hardness and wear resistance [17]. In another study, Paraye et al. reported an increase in wear resistance by in-situ growth of titanium carbide (TiC) particles using tungsten inert gas (TIG) arcing [13]. Laser surface heat treatment is also an effective method for enhancing the wear resistance of AISI 8620 steel. This process focuses laser energy on a small area, resulting in increased surface microhardness and reduced surface roughness, thereby collectively improving wear resistance [19]. Gorlenko et al. (2019) employed electro-mechanical treatment (EMT) technology, which

involves controlling current density during processing to optimize the surface layer quality of AISI 8620 steel, thereby enhancing wear resistance [20]. However, these methods often involve high equipment costs, complex process steps, and material-geometry limitations, necessitating alternative solutions. In this context, pack boriding emerges as an economical and feasible surface hardening technique [21-23]. Pack boriding, performed in a high-temperature boriding environment, involves boron diffusion into the steel surface to form hard boride layers (FeB/Fe₂B). These layers exhibit outstanding wear resistance with hardness values ranging from 1500 to 2000 HV, along with additional benefits such as low friction coefficients and enhanced corrosion resistance. The method's low equipment investment requirements, suitability for mass production, and ability to provide uniform coatings even on complex geometries further increase its industrial appeal [14, 22, 23]. In this study, AISI 8620 steel was borided using commercial Ekabor II boron powder. The microstructure, layer thickness, surface hardness, and wear behavior of the resulting boride layer were investigated.

Given the industrial necessity for a cost-effective and scalable solution to enhance the wear resistance of commonly used steels, such as AISI 8620, this study is motivated by the need to systematically evaluate pack boriding as a viable alternative to more complex and expensive surface engineering techniques. Unlike other surface modification methods, pack boriding offers a cost-effective, scalable, and geometry-independent approach, making it highly relevant for industrial applications. In this context, the main objective of the present study is to investigate the microstructural evolution, layer thickness, surface hardness, and wear performance of borided AISI 8620 steel, thereby establishing a clear relationship between the boride layer characteristics and the resulting mechanical and tribological behavior. The findings of this study are expected to provide valuable data and a robust reference for industry practitioners seeking to implement pack boriding to extend the service life of AISI 8620 components operating in severe abrasive and adhesive wear environments.

2 MATERIAL AND METHOD

In this study, AISI 8620 steel, the chemical composition of which is presented in Table 1, was used in the form of specimens with dimensions of Ø24 × 9 mm. The boriding process was performed by the pack boriding method utilizing commercial Ekabor II powder. The commercial Ekabor II powder has a nominal chemical composition of 5% B₄C, 5% KBF₄, and 90% SiC, and was used as the boriding agent. The specimens were placed inside a cylindrical stainless steel crucible filled with Ekabor II powder. The furnace was preheated to 900°C prior

to the placement of the crucible, and the boriding treatment was carried out at this temperature for a duration of 5 h. After this process, the samples were allowed to cool naturally to room temperature. Following boriding, the surfaces of the specimens were ground and polished using silicon carbide abrasive papers ranging from 240 to 1000 grit, followed by polishing with 0.1 μ m alumina suspensions. Subsequently, the samples were etched using a 3% Nital solution to reveal the microstructure. The thickness of the boride layer was determined as the arithmetic mean of measurements taken at 10 different locations using an optical microscope equipped with a measurement device. The microstructural examinations of the worn regions of the borided specimens were conducted using a scanning electron microscope. In addition, the elemental distributions within the borided layers were analyzed by energy-dispersive X-ray spectroscopy. Phase analysis of the borided surface was performed via X-ray diffraction employing CuK α radiation (λ = 1.5418 Å) over a 2 θ range of 20° to 90°. Finally, microhardness measurements were carried out using the Vickers hardness tester under a load of 50 g. Measurements were taken at regular intervals, with at least 5 readings obtained for each sample, and the average hardness value was subsequently calculated.

Table 1. The chemical composition of AISI 8620 (wt. %)

| Material | C | Cr | Ni | Si | Mn | Mo | S | P |
|-----------|------|------|------|------|------|------|-------|-------|
| AISI 8620 | 0.18 | 0.45 | 0.52 | 0.25 | 0.80 | 0.20 | 0.035 | 0.030 |

The wear tests were conducted at room temperature on the borided specimens. Wear tests were performed using a ball-on-disk system and WC-Co balls with a diameter of 8 mm were used. A separate wear element was used for each test to eliminate errors arising from surface degradation. The wear tests were carried out in dry sliding conditions at room temperature, under a load of 10 N, at rotational speeds of 300, 450, and 600 rpm, and over sliding distances of 250, 500, 750, 1000, 1500, and 2000 meters. Each wear test condition (combination of speed and distance) was repeated twice to ensure reproducibility. All test parameters are listed in Table 2.

Table 2. Test parameters

| Applied load (N) | Sliding distance (m) | RPM | | | |
|---------------------|---------------------------------|-----|-----|-----|--|
| 10 | 250, 500, 750, 1000, 1500, 2000 | 300 | 450 | 600 | |

Before and after the wear tests, each specimen and wear element were cleaned with alcohol. The wear volume of the specimens was determined by multiplying the cross-sectional area of the wear tracks, obtained using a Taylor Rugosimeter, by the circumference of the wear track. The wear rate was calculated using the following formula (1):

$$WR = \frac{WV}{SDxAL} \tag{1}$$

Where WR is the wear rate (mm³N⁻¹m⁻¹), WV is the wear volume (mm³), SD is the sliding distance (m) and AL is the applied load (N). The coefficients of friction were determined as a function of sliding distance using a program associated with the system. Based on the results of the wear tests, graphs showing the relationships between boriding temperature, sliding speed, coefficient of friction, surface roughness, and wear rate were plotted.

3 RESULTS AND DISCUSSION

3.1 Microstructure and mechanical properties

Figure 1 illustrates the cross-sectional microstructure of AISI 8620 steel subjected to pack boriding at 900 °C for 5 h, as observed under an optical microscope using commercial Ekabor II powder. As a result of the boriding process, saw-tooth shaped boride layers were formed on the specimens. A boride layer thickness of 78±2 μm was achieved in the steel cross-section. In the optical microscopy analysis, the dark regions represent the FeB phase, while the light-colored regions correspond to the Fe₂B phase. The characteristic saw-tooth or acicular morphology of the boride layer, evident in Figure 1, is a result of the anisotropic growth of boride crystals. It is well-documented in the literature that boriding of steels results in the formation of FeB and Fe₂B phases, which can be distinctly identified through microstructural examinations [24-26].

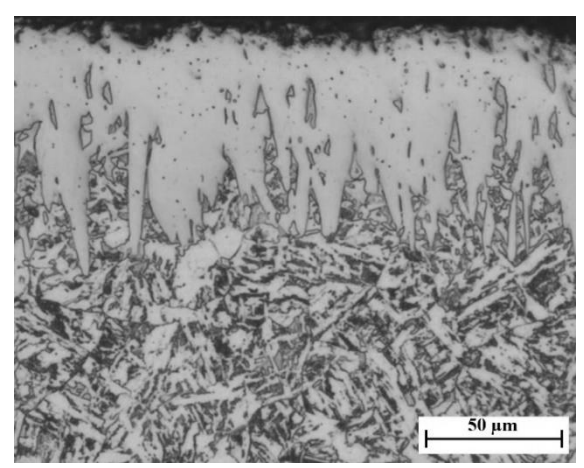


Figure 1. Cross-sectional wiev of the borided AISI8620 steel.

The boride layer thickness of AISI 8620 steel borided with Ekabor II powder was calculated as the arithmetic mean of measurements taken at 20 different locations using an apparatus connected to an Olympus BX-60 optical microscope. A boride layer thickness of 86 µm was obtained for AISI 8620 steel borided at 900°C for 5 h. The XRD results of the borided AISI 8620 steel are provided in Figure 2. As a result of the boriding process applied to AISI 8620 steel with commercial Ekabor II boron powder at 900°C for 5 h, a dual-phase (FeB + Fe₂B) boride layer was formed. The formation of a dual-phase (FeB + Fe₂B) layer at 900°C for 5 hours using Ekabor II powder is directly influenced by the high chemical activity of the boriding medium. Ekabor II contains KBF₄, which acts as an activator. This high boron potential at the material's surface promotes the formation of the boron-rich FeB phase atop the more desirable Fe₂B phase. While a single-phase Fe₂B layer is often preferred due to its lower brittleness, the process parameters and activator content in commercial powders like Ekabor II frequently result in a thin FeB outer layer, as observed in this study and is consistent with findings from other studies using activated boriding powders.

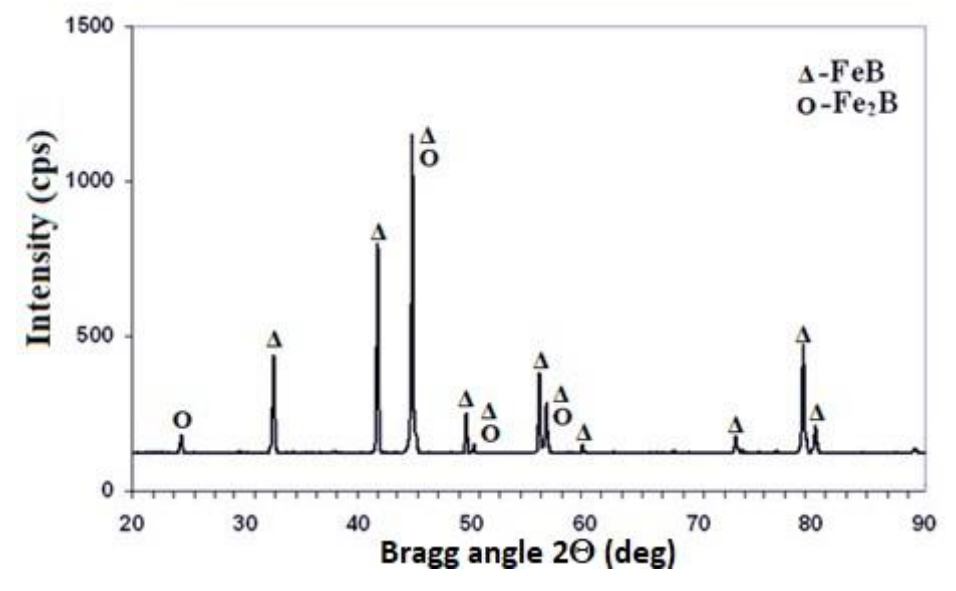


Figure 2. XRD results of borided AISI8620 steel.

The hardness distribution from the surface towards the interior of AISI 8620 steel was determined using a Vickers microhardness tester under an applied load of 50 g, and the corresponding results are presented in Figure 3. The high surface hardness is attributed to the FeB and Fe₂B phases formed as a result of the pack boriding process with Ekabor II powder. It is well known that the FeB and Fe₂B phases exhibit high hardness values [27, 28].

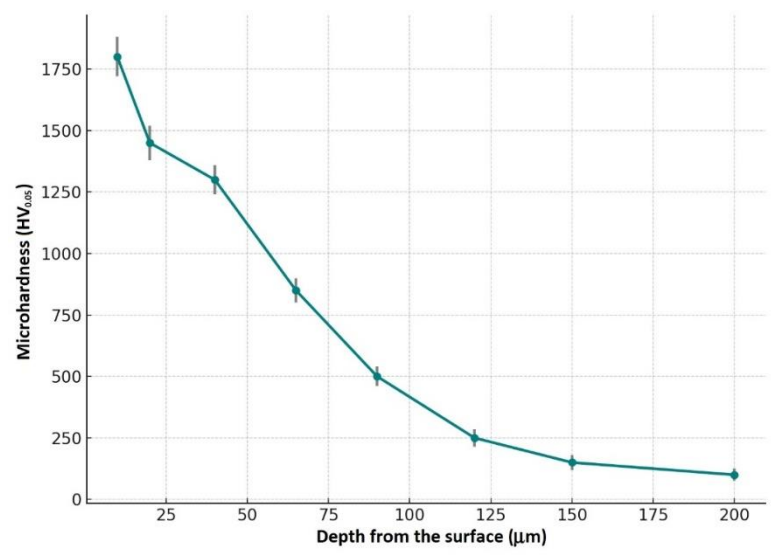


Figure 3. The cross sectional microhardness values varying with the depth for borided AISI 8620 steel.

3.2 Tribological properties

Figure 4 presents the coefficient of friction values for borided AISI 8620 steel at sliding distances of 250, 500, 750, 1000, 1500, and 2000 meters under rotational speeds of 300, 450, and 600 rpm. Generally, similar coefficient of friction values were observed at sliding speeds corresponding to 300 and 450 rpm, whereas a decrease in the coefficient of friction was noted as the speed increased to 600 rpm. This decrease can be attributed to the formation of oxides on the specimen surfaces due to surface heating caused by friction at higher sliding speeds[29]. When we examine the friction coefficient values depending on the distance traveled, we observe an increase up to 1000 meters and a slight decrease after 1000 meters. This is thought to be due to the lubricating properties of the boron layer. Similar results have been observed in the literature [29, 30].

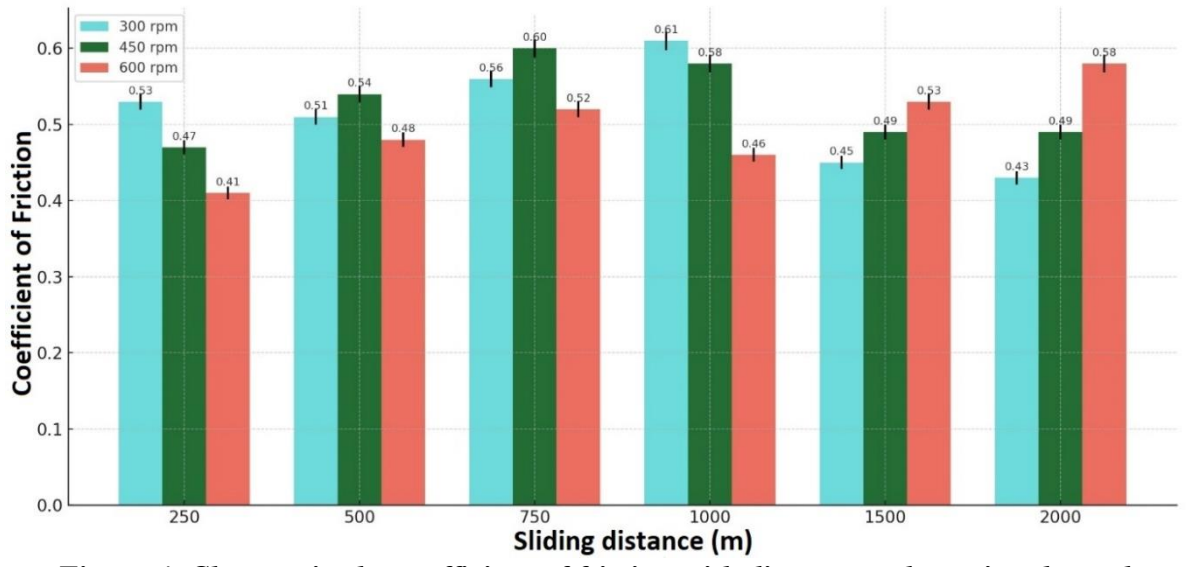


Figure 4. Changes in the coefficient of friction with distance and rotational speed.

It was observed that at 300 and 450 rpm, the wear depth increased at similar rates; however, when the rotational speed was elevated to 600 rpm, the wear depth values initially decreased up to a certain distance, followed by an increase beyond that point. This behavior may be attributed to the formation of an oxide film on the specimen surfaces as a result of frictional heating at high sliding speeds. The oxide film serves as a protective layer against friction and wear. Nevertheless, as the wear distance increases, the oxide film grows to a critical thickness, leading to the formation of protrusions and subsequent fracture. The resulting hard debris acts as a third body, initiating and exacerbating abrasive wear. With increasing wear distance, oxide particles progressively contributed to greater wear depth, particularly at longer sliding distances. An increase in wear rates was observed with increasing wear distance and rotational speed. The lowest wear rate was recorded for the specimen tested at 250 meters and 300 rpm, while the highest wear rate was observed for the specimen tested at 2000 meters and 600 rpm.

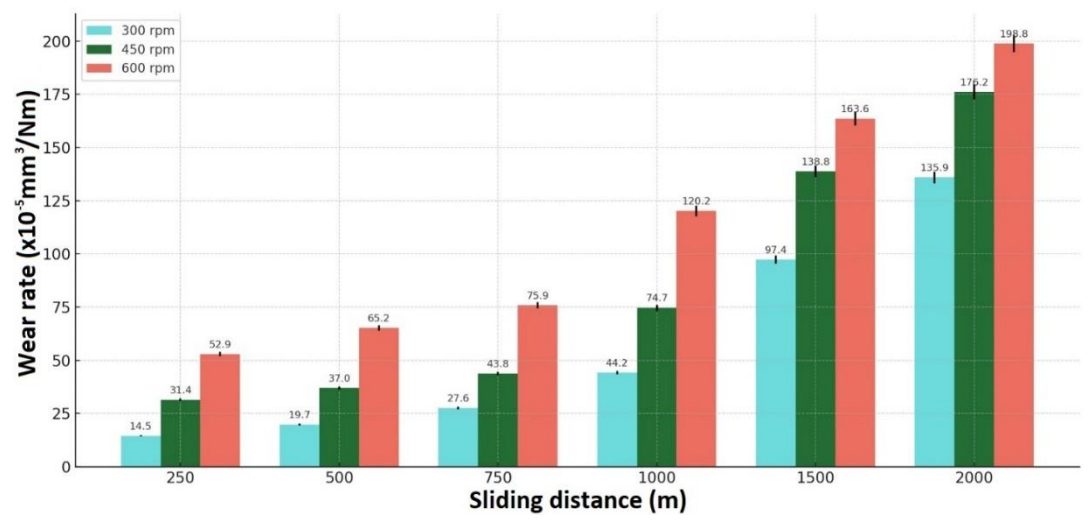


Figure 5. Variation of wear depth at different distances and rotational speeds.

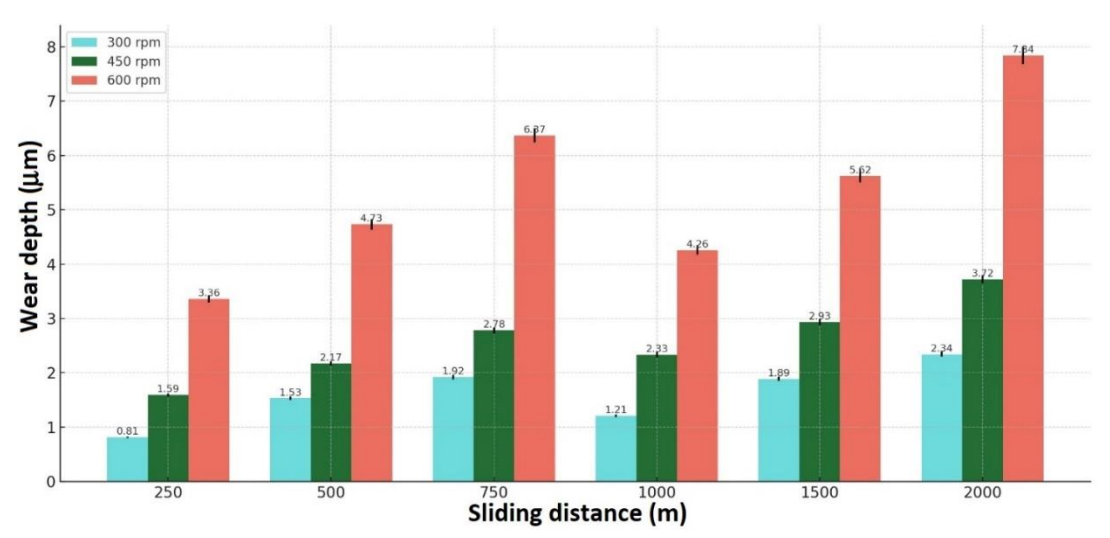


Figure 6. Changes in wear rate with respect to distance and rotational speed.

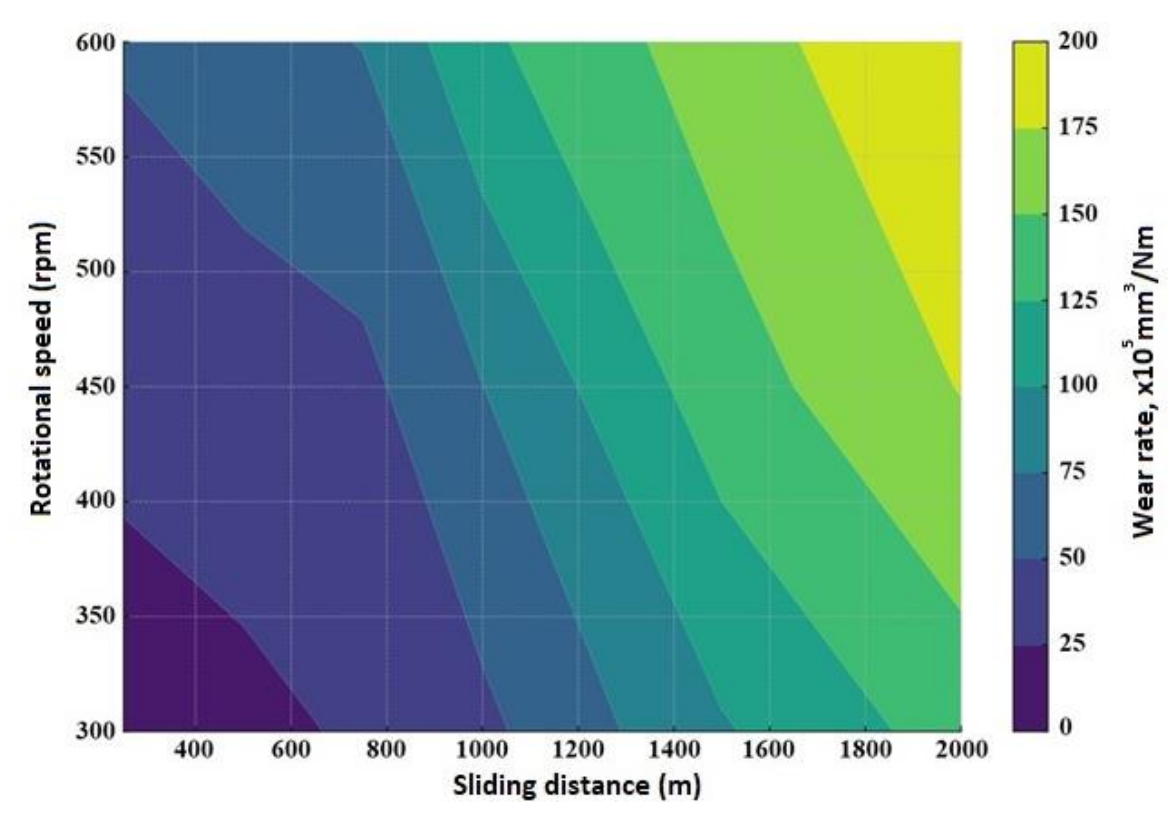


Figure 7. Variation of wear rate at different rotational speeds and wear distances.

Figure 8 a-f illustrates the SEM microstructures of the wear surfaces of AISI 8620 steel specimens worn at 600 rpm over different sliding distances, 250 m, 500 m, 750 m, 1000 m, 1500 m and 2000 m respectively. In this figure, it is observed that the wear surfaces exhibit rough and coarse wear debris and particles. With increasing sliding intensity, the coarse particles are transformed into finer debris, leading to a reduction in wear severity (as shown in Figure 6). In Figures 8d and 8f, oxide residues, abrasive scratches, and delamination layers (wear-induced layers) are identified on the wear surfaces of the specimens. Additionally, in Figures 8c-f, microcracks are observed along the wear track of the specimens.

The wear test results showed that wear rates increased as the sliding distance (path length) increased. This is expected. However, the lower wear rates at low speeds are thought to be due to both the lower friction speed and the lower heat generated during friction, resulting in more wear particles being trapped between the abrasive ball and the sample. At high wear speeds, more hard boride particles from the surface are trapped between the abrasive ball and the sample, causing more scratching and wear on the boride surfaces. Furthermore, the frictional heat generated by the fast rotational speed is also high, which leads to the rapid formation of hard oxide particles in the wear zone. Studies on wear rates in the literature have also encountered these situations [24, 31, 32].

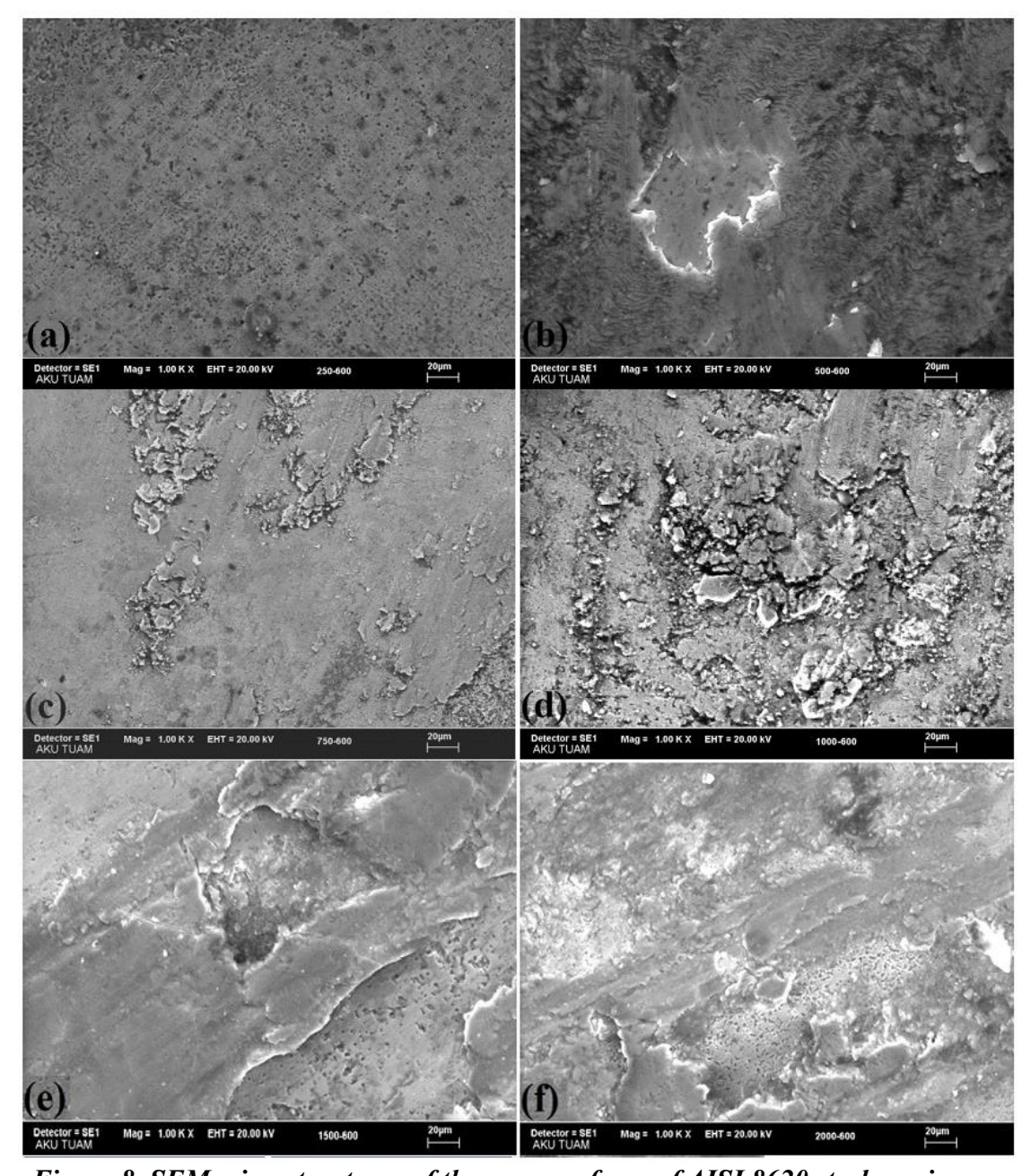


Figure 8. SEM microstructures of the wear surfaces of AISI 8620 steel specimens.

With increasing sliding distance, it was observed that the wear intensified, leading to delamination in the layers. Figure 9 presents the EDX analyses obtained from Figures 8d and 8f. The EDX analyses revealed the formation of Fe-based oxide layers on the worn specimen surfaces due to frictional heat. Additionally, it was observed that the oxide layers extended and aligned along the sliding direction on the wear track. Gunes [30] studied the wear of borided and plasma-nitrided AISI W9Mo3Cr4V high-speed steel and reported the presence of oxide layers formed due to frictional heat on the wear surfaces of borided steel. They found that these oxide layers extended along the wear track and significantly influenced the wear behavior of borided steels [30].

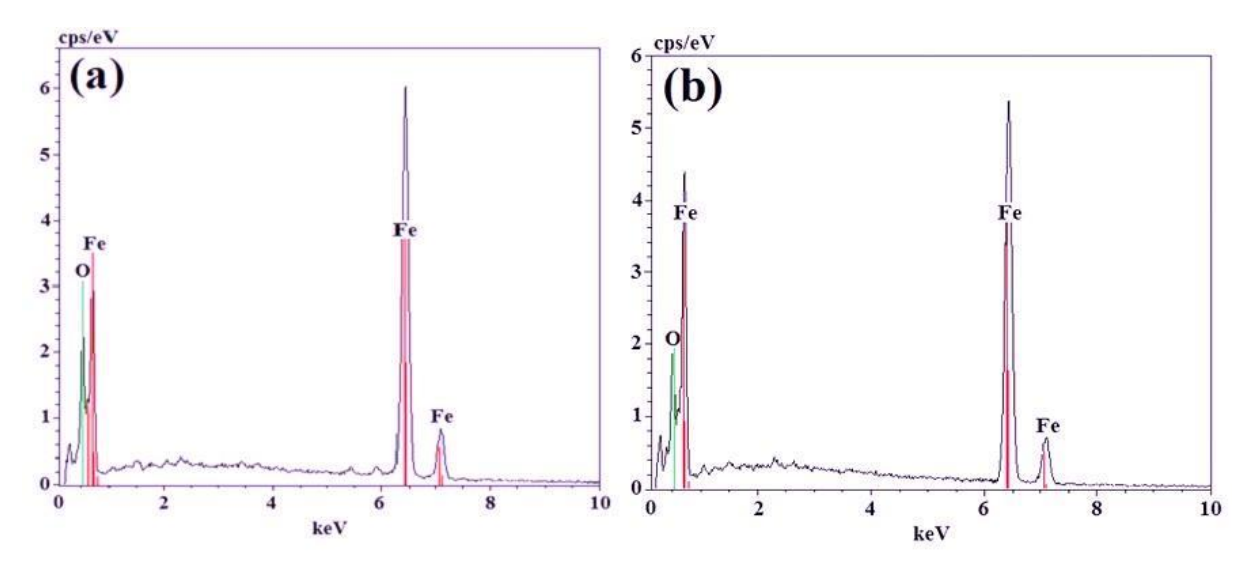


Figure 9. EDX analyses of borided AISI 8620 steels tested at 600 rpm with a sliding distance of (a) 1000 m and (b) 2000 m.

4 **CONCLUSIONS**

The conclusions drawn from the current study on wear properties of borided AISI8620 steel are given below:

- 1. The box boriding process of AISI 8620 steel was successfully conducted using commercial Ekabor II boron powder at 900°C for 5 h, resulting in an approximately $78\pm2~\mu m$ thick boride layer.
- 2. Metallographic examinations revealed a distinct separation between the coating/matrix interface and the matrix, and the boride layer was observed to have a columnar structure.
- 3. X-ray diffraction analysis confirmed the formation of a dual-phase structure (FeB + Fe₂B) as a result of box boriding with Ekabor II powder.
- 4. A hardness value of 1768 HV_{0.05} was achieved following the box boriding process with commercial Ekabor II powder at 900°C for 5 h.
- 5. The wear tests conducted on AISI 8620 steel at different sliding distances and rotational speeds showed that both the sliding distance and rotational speed increased the wear rate.
- 6. During the wear tests, it was observed that at lower sliding distances, the rotational speed led to a reduction in the coefficient of friction, whereas, at longer sliding distances, it contributed to an increase in wear severity.

This study was limited to a single boriding treatment parameters. Future work could explore a range of temperatures and times to optimize the boride layer (e.g., minimizing the brittle FeB phase) and correlate its specific properties (thickness, phase ratio) with wear performance. Furthermore, conducting tests under lubricated conditions would provide valuable data for real-world gear applications. Finally, the use of more advanced techniques like nanoindentation to map the mechanical properties across the boride layer and profilometry to quantitatively analyze wear track topography would provide deeper insights into the wear mechanisms.

Conflict of Interest Statement

There is no conflict of interest between the authors.

Statement of Research and Publication Ethics

The study is complied with research and publication ethics.

Acknowledgement

This study was financially supported by the Scientific Research Projects Unit of Giresun University under project number FEN-BAP-A-2990224-13.

Artificial Intelligence (AI) Contribution Statement

This manuscript was entirely written, edited, analyzed, and prepared without the assistance of any artificial intelligence (AI) tools. All content, including text, data analysis, and figures, was solely generated by the authors.

Contributions of the Authors

Selçuk Atasoy: Writing, analysis

Hasan Onur Tan: Writing, analysis

Sıtkı Aktaş: Methodology, writing

Hakan Adatepe: Methodology, writing

İbrahim Güneş: Conceptualization, methodology, writing

REFERENCES

- [1] M. Musa, A. G. Mohammed, and A. Muhammad, "Wear properties of boron added high strength low alloy (HSLA) SAE 8620 steel," *Journal of Metals, Materials and Minerals*, vol. 28, no. 1, 2018.
- [2] R. Sankaran, D. Rajamani, S. Natarajan, and K. Thirugnanasambantham, "Sliding wear behaviour and its mechanisms of carbonitrided AISI 8620 steel at 100 C under unlubricated conditions," *Surface Engineering*, vol. 33, no. 1, pp. 42-48, 2017.
- [3] J. An, Z. Su, X. Gao, Y. Yang, and S. Sun, "Corrosion characteristics of boronized AISI 8620 steel in oil field water containing H₂S" *Prot Met Phys Chem*+, vol. 48, pp. 487-494, 2012.
- [4] S. Tajmiri, W. Haider, and I. Shabib, "Effect of Heating Rate on Microstructure and Corrosion Resistance of Quenched and Tempered 8620 Low Carbon Alloy Steel," *Corrosion and Materials Degradation*, vol. 5, no. 3, pp. 370-386, 2024.
- [5] E. H. Sabuz, M. Noor-A-Alam, W. Haider, and I. Shabib, "Improving the mechanical and electrochemical performance of additively manufactured 8620 low alloy steel via boriding," *Corrosion and Materials Degradation*, vol. 4, no. 4, pp. 623-643, 2023.
- [6] E. Boyle, D. Northwood, R. Bowers, X. Sun, and P. Bauerle, "The effects of initial microstructure and heat treatment on the core mechanical properties of carburized automotive steels," in *Materials Forum*, vol. 32, pp. 44-54, 2008.
- [7] M. A. Erden and F. Aydın, "Wear and mechanical properties of carburized AISI 8620 steel produced by powder metallurgy," *International Journal of Minerals, Metallurgy and Materials*, vol. 28, pp. 430-439, 2021.
- [8] S. Hong, H. Lin, C. Yang, L. Tseng, and K. Lin, "Effects of heat treatment and composition modification on SAE 8620 steels," in *Materials science forum*, vol. 539: pp. 4452-4457, 2007.
- [9] K. Genel and M. Demirkol, "Effect of case depth on fatigue performance of AISI 8620 carburized steel," *International Journal of Fatigue*, vol. 21, no. 2, pp. 207-212, 1999.
- [10] P. Ghosh and N. Dhokey, "Refinement of tempered martensite structure and its effect on wear mechanism in SAE 8620," *Tribology-Materials, Surfaces & Interfaces*, vol. 10, no. 4, pp. 178-184, 2016.
- [11] O. Kapustynskyi and L. Golovko, "Effects of laser cladding and treatment methods on wear resistance in heavy-loaded units," *International journal of multidisciplinary research updates.*, vol. 7, no. 1, pp. 17-26, 2024.
- [12] N. Bhadauria, S. Pandey, and P. Pandey, "Wear and enhancement of wear resistance—A review," *Materials Today: Proceedings*, vol. 26, pp. 2986-2991, 2020.
- [13] N. K. Paraye, S. P. Neog, P. K. Ghosh, and S. Das, "Surface modification of AISI 8620 steel by in-situ grown TiC particle using TIG arcing," *Surface and Coatings Technology*, vol. 405, p. 126533, 2021.
- [14] I. Gunes, I. Yildiz, and A. G. Çelik, "Wear Resistance and Characterization of Borided Ni-Based Alloys," *Powder Metallurgy and Metal Ceramics*, vol. 60, no. 11, pp. 717-726, 2022.
- [15] M. Erdogan and S. Tekeli, "The effect of martensite volume fraction and particle size on the tensile properties of a surface-carburized AISI 8620 steel with a dual-phase core microstructure," *Mater Charact*, vol. 49, no. 5, pp. 445-454, 2002.
- [16] R. Ortega-Álvarez, M. T. Hernández-Sierra, L. D. Aguilera-Camacho, M. G. Bravo-Sánchez, K. J. Moreno, and J. S. García-Miranda, "Tribological performance of 100Cr6/8620 steel bearing system under green oil lubrication," *Metals*, vol. 12, no. 2, p. 362, 2022.
- [17] R. M. Triani, F. E. Mariani, L. F. D. A. Gomes, P. G. B. De Oliveira, G. E. Totten, and L. C. Casteletti, "Improvement of the tribological characteristics of AISI 8620, 8640 and 52100 steels through thermoreactive treatments," *Lubricants*, vol. 7, no. 8, p. 63, 2019.
- [18] A. Krelling, C. Da Costa, J. Milan, and E. Almeida, "Micro-abrasive wear mechanisms of borided AISI 1020 steel," *Tribology International*, vol. 111, pp. 234-242, 2017.
- [19] S. K. Yaseen, H. F. Oleiwi, and H. Al-Taay, "Wear Resistance Improvement of Alloy Steel Using Laser Surface Treatment," *Iraqi Journal of Industrial Research*, vol. 9, no. 3, pp. 57-62, 2022.

- [20] A. Gorlenko, S. Davydov, M. Y. Shevtsov, and D. Boldyrev, "Wear-resistance increase of friction surfaces of steel machine parts by electro-mechanical hardening," *Steel in Translation*, vol. 49, pp. 800-805, 2019.
- [21] E. Hernández-Sánchez *et al.*, "Tribological and Mechanical Behavior of Automotive Crankshaft Steel Superficially Modified Using the Boriding Hardening Process," *Coatings*, vol. 14, no. 6, p. 716, 2024.
- [22] H. O. Tan, S. Atasoy, and S. Aktaş, "The Effect of Boriding Temperature and Time on the Structural and Mechanical Properties of M42 Steel," *Türk Doğa ve Fen Dergisi*, vol. 13, no. 2, pp. 1-5, 2024.
- [23] I. Gunes, "Tribological Behavior and Characterization of Borided Cold-Work Tool Steel," *Materials and Technology*, vol. 48, no. 5, pp. 765-769, 2014.
- [24] I. Gunes, "Wear behaviour of plasma paste boronized of AISI 8620 steel with borax and B₂O₃ paste mixtures," *J Mater Sci Technol*, vol. 29, no. 7, pp. 662-668, 2013.
- [25] A. Milinovic, S. Simunovic, M. Keddam, and M. M. Butkovic, "Boronizing Kinetics of 30CrNiMo8 Steel," *Technical Gazette*, vol. 32, no. 1, pp. 176-181, 2025.
- [26] S. U. Bayça and H. Efe, "Coating of AISI 8620 steel by boriding process: kinetic modeling, empirical formula and error analysis," *Metall Res Technol*, vol. 122, no. 3, 2025.
- [27] C. Pacheco, J. L. Jeronimo, A. P. Krelling, C. E. da Costa, and J. C. G. Milan, "Influence of boriding treatment on the mechanical properties of Monel 400," *Results Surf Interf*, vol. 18, 2025.
- [28] I. Gunes and I. Yıldız, "Investigation of adhesion and tribological behavior of borided AISI 310 stainless steel," *Matéria (Rio de Janeiro)*, vol. 21, no. 1, pp. 61-71, 2016.
- [29] I. Gunes and A. Dalar, "Effect of sliding speed on friction and wear behaviour of borided gear steels," *Journal of the Balkan Tribological Association*, vol. 19, no. 3, pp. 325-339, 2013.
- [30] I. Gunes, "Effect of sliding speed on the frictional behavior and wear performance of borided and plasmanitrided W9Mo3Cr4V high-speed steel," *Materials and Technology*, vol. 49, no. 1, pp. 111-116, 2015.
- [31] R. Tyagi, D. S. Xiong, and J. L. Li, "Effect of load and sliding speed on friction and wear behavior of silver/h-BN containing Ni-base P/M composites," *Wear*, vol. 270, no. 7-8, pp. 423-430, 2011.
- [32] Y. Kanca, "Effects of normal load and sliding distance on the dry sliding wear characteristics of Invar-36 superalloy," *Erzincan University Journal of Science and Technology*, vol. 16, no. 1, pp. 258-272, 2023.